Carbohydrate Polymers 84 (2011) 566–570

Contents lists available at ScienceDirect

Carbohydrate Polymers

journal homepage: www.elsevier.com/locate/carbpol

Synthesis and optical characterization of ZnS–sodium carboxymethyl cellulose nanocomposite films

J.F. Luna-Martínez[a,b], D.B. Hernández-Uresti[a,b], M.E. Reyes-Melo[a,b], C.A. Guerrero-Salazar[a,b], V.A. González-González[a,b], S. Sepúlveda-Guzmán[a,b,*]

[a] Facultad de Ingeniería Mecánica y Eléctrica, UANL, Av. Universidad s/n, Cd. Universitaria, San Nicolás de los Garza, N.L. 66450, Mexico
[b] Centro de Innovación, Investigación y Desarrollo en Ingeniería y Tecnología, UANL Nueva Carretera al Aeropuerto Internacional Monterrey Km 10-PIIT, Apodaca, N.L. 66600, Mexico

ARTICLE INFO

Article history:
Received 8 September 2010
Received in revised form 6 December 2010
Accepted 7 December 2010
Available online 14 December 2010

Keywords:
Carboxymethyl cellulose
ZnS
Optical properties
Quantum dots

ABSTRACT

In this work, the synthesis and characterization of ZnS–sodium carboxymethyl cellulose nanocomposite films were studied. The film was prepared by casting after the *in situ* precipitation of ZnS in sodium carboxymethyl cellulose (NaCMC) aqueous solution. The *in situ* method avoids nanoparticles aggregation and improves its dispersion. The resulting nanocomposite was characterized by X-ray diffraction (XRD), Fourier transformed infrared spectroscopy (FTIR) and transmission electron microscopy (TEM). The results showed that ZnS nanoparticles with a blende structure and a particle size in the range of few nanometers are well dispersed in the sodium carboxymethyl cellulose films. Optical properties were analyzed by using UV–vis spectroscopy and photoluminescence spectroscopy (PL). The resulting nanocomposite films showed optical transmission between 50% and 90% influenced by the amount of ZnS nanocrystals into the nanocomposite films. The PL spectra of the nanocomposite films exhibits a broad visible emission band centered at 445 nm under UV light excitation (λ = 320 nm). These luminescent films might have a potential application in security paper by using an optical signature.

1. Introduction

Semiconductor nanocrystals, usually known as quantum dots (QDs), exhibit very interesting optical properties and have attracted interest due to their size dependant properties, stemming from their quantum confinement effects and large surface area (Kuiri et al., 2007; Mu, Gu, & Xu, 2005). ZnS has a direct wide band-gap energy ranging from 3.5 to 3.7 eV and has became very attractive due to its low toxicity when is compared to other semiconductors (Velumani & Ascencio, 2004). These properties make ZnS suitable for several applications as bioelectronics and light emitting devices (Rosseti, Ellison, Gibson, & Brus, 1984). A wide variety of synthesis methods have been used to prepare ZnS nanocrystals such as sol–gel (Arachchige & Brock, 2007; Hebalkar et al., 2001), solid state (Calandra, Longo, & Liveri, 2003), micro-wave irradiation (Zhu, Zhou, Xu, & Liao, 2001) and ultrasonic irradiation (Xu, Ji, Lin, Tang, & Du, 1998). In addition, physical methods such as sputtering (Kuiri et al., 2007) and thermal evaporation (Velumani & Ascencio, 2004) techniques have also been studied in detail to prepare ZnS films. Semiconductor nanoparticles dispersed into a flexible matrix are required due to the advances in organic based electronic devices.

During the last decade several research works about the incorporation of QDs with a high photoluminescent properties dispersed in polymers and cellulose or cellulose derivatives polymers have been previously investigated (Generalova et al., 2009; Gruzintsev et al., 2009; Guo, Chen, & Chen, 2007; Li et al., 2009; Pandey & Pandey, 2009). The increasing interest in the preparation of such materials arises from their potential application in security paper or sheets with optical signatures. Abitbol et al. reported the preparation of CdSe/ZnS semiconductor nanoparticles in cellulose triacetate (CTA) by mixing a QDs dispersion with a CTA solution. A clear film was obtained by solvent casting process. The nanoparticle dispersion in CTA was increased by adding hydrophobic ligands that passivated QDs surface (Abitbol & Gray, 2007). In addition, the preparation of fluorescent cellulose nanocomposite films and fluorescent hydrogels by mixing alkali soluble cellulose and QDs dispersed in water has also been reported (Chang, Peng, Zhang, & Pang, 2009; Qi, Chang, & Zhang, 2009). In a different approach, the *in situ* precipitation method has been an efficiency technique to manipulate and to process nanoparticles in technologically useful formulations based on nanocomposites. During this process the nanoparticles grow in the polymer matrix, whose molecules play a dual role; first stabilize and isolate the generated nanoparticles avoiding aggregation and after drying,

* Corresponding author at: Facultad de Ingeniería Mecánica y Eléctrica, UANL, Av. Universidad s/n, Cd. Universitaria, San Nicolás de los Garza, N.L. 66450, Mexico. Tel.: +52 81 1340 4020; fax: +52 81 1052 3321.
E-mail address: selene.sepulvedagz@uanl.edu.mx (S. Sepúlveda-Guzmán).

0144-8617/$ – see front matter © 2010 Elsevier Ltd. All rights reserved.
doi:10.1016/j.carbpol.2010.12.021

serve as a confined medium that protects the nanoparticles surface (Rozenberg & Tenne, 2008). Ruan, Huang, and Zhang (2005) reported the preparation of QD/polymer composite films by using the *in situ* precipitation of CdS nanoparticles in cellulose solution and the subsequent casting of the resulting CdS/cellulose in NaOH/urea aqueous solution. A novel approach, reported the preparation of hydrogel–silver nanocomposites via *in situ* in the presence of three different polymers: gum acacia (GA), sodium carboxymethyl cellulose (NaCMC) and starch (SR) to control sized nanoparticles (Vimala, Samba Sivudu, Murali Mohan, Sreedhar, & Mohana Raju, 2009).

Sodium carboxymethyl cellulose (NaCMC) is a cellulose derivative obtained through the reaction between a cellulose alkali with sodium monochloroacetate. NaCMC is an anionic water soluble polymer and has been gained interest due to its properties, such as high transparency in the spectral region where the QDs emit and film forming ability. NaCMC has been widely used in several applications such as drug delivery, textile printing and paper industry, among others. Recently a lot of interest has been paid in the synthesis of hybrid nanocomposites based on NaCMC with potential application in the paper industry. Carboxymethyl cellulose–copper complexes [CMC–Cu(II)] were prepared as paper additive and it was found that durability and the strength properties of wood pulp paper sheet were increased (Basta & El-Saied, 2008). On the other hand optical properties such as the brightness and opacity of the paper sheets were markedly enhanced by adding a functional formulation based on CMC-calcium carbonate fillers nanocomposites (Shen, Song, Qiana, & Yang, 2010). In this work, we report the *in situ* precipitation of ZnS nanoparticles in NaCMC as polymer matrix. NaCMC acts as stabilizing agent during ZnS synthesis and as matrix after subsequent casting of the ZnS–NaCMC aqueous solution providing a confined medium for ZnS particle growing resulting in a uniform size. The ZnS–NaCMC nanocomposite solution gives a transparent film in visible region after casting. The resulting nanocomposite films were characterized by X-ray diffraction (XRD), Fourier transformed infrared spectroscopy (FTIR) and transmission electron microscopy (TEM). In addition, the optical properties of the nanocomposites were studied by UV–vis spectroscopy and photoluminescence spectroscopy.

2. Experimental

2.1. Materials

Reagent grade zinc nitrate hexahydrate ($Zn(NO_3)_2{\cdot}6H_2O$) and sodium sulfide nonahydrate ($Na_2S{\cdot}9H_2O$) were acquired from Fermont, Mexico, and sodium carboxymethyl cellulose (NaCMC) (heavy metals $\leq$ 0.002%, and DS = 0.7), was purchased from Aldrich all reagents were used as received without additional purification.

2.2. Preparation of ZnS–NaCMC nanocomposites

In a typical process 0.7312 g of NaCMC were dissolved in 30 mL of deionized water at room temperature until a clear solution was formed. 0.1487 g of zinc nitrate were dissolved in 5 mL of deionized water and added to the NaCMC water solution and kept under stirring for 30 min. 0.12 g of sodium sulfide were dissolved in 5 mL of deionized water and added drop-wise to the zinc nitrate and NaCMC solution at room temperature. The mixture was kept under stirring at room temperature until the solution turns milky white. The solution of ZnS–NaCMC nanocomposite was dialyzed using standard cellulose dialysis tubing. Finally the ZnS–NaCMC nanocomposite solution was casted into a petri dish and dried at 60 °C under vacuum for 24 h. Additional experiments varying the weight % ratio of $Zn(NO_3)_2/Na_2S$/NaCMC were carried out. The resulting samples were denoted as S2, S3 and S4 for the 15/12/73, 29/24/47 and 44/36/20 wt% ratio respectively.

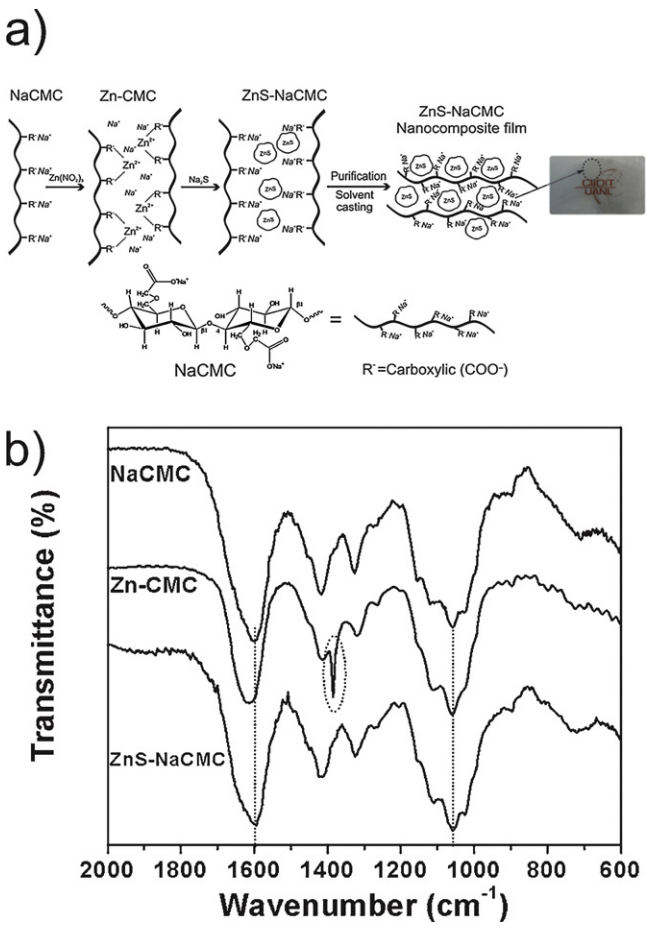

Fig. 1. (a) Scheme for the ZnS *in situ* precipitation process using NaCMC as polymer matrix and (b) FTIR spectra of as received NaCMC, zinc–CMC sample and ZnS–NaCMC nanocomposite.

2.3. Characterization

Fourier transformed infrared spectroscopy (FTIR) was performed by using a Nicolet FT-IR Spectrometer 6700. X-ray diffraction patterns were acquired using a Bruker Advanced solutions D8 equipment, provided with a Cu tube with Kα radiation at 1.54 Å, scanning in the 25–75° 2θ range with increments of 0.03° and a swept time of 8 s. The semiconductor nanoparticles were analyzed by transmission electron microscopy (TEM) on JEOL 2010F at 200 kV. Samples were dispersed in water at room temperature and sonicated. Aliquots were dropped on 3 mm diameter carbon film copper grids. The optical characterization of ZnS–NaCMC nanocomposite was carried out by UV–vis spectroscopy in a PerkinElmer Lambda 35 UV–vis system. The photoluminescence (PL) characterization was performed at room temperature on a PerkinElmer L55 Fluorescence Spectrometer under an excitation of 320 nm from a 7.3 W Xe lamp.

3. Results and discussion

3.1. Structure characterization

ZnS nanoparticles were *in situ* synthesized into the sodium carboxymethyl cellulose (NaCMC). Fig. 1a shows the proposed mechanism for the *in situ* precipitation of ZnS nanoparticles into

NaCMC matrix. During this process NaCMC and zinc nitrate were dissolved in water, and a Zn–CMC complex was formed through the electrostatic interaction between Zn^{2+} ions and carboxylic groups in CMC. Once the Na_2S solution was added to the mixture, the reaction between Zn^{2+} and S^{2-} ions was immediate forming the ZnS nanoparticles. The reaction was evidenced by a change in the color form clear to milky white. FTIR analysis was performed in order to study the *in situ* precipitation synthesis of ZnS and the interactions between the semiconductor nanoparticles and the CMC matrix. Fig. 1b shows the FTIR spectra of the NaCMC, Zn–CMC and ZnS–NaCMC samples. The FTIR spectrum of the NaCMC displays the asymmetric stretching vibration band of ether groups at 1058 cm^{-1} and the symmetric and asymmetric modes of stretching vibration of carboxylic groups (COO–) at 1600 and 1417 cm^{-1} respectively. In addition, a FTIR spectrum of the NaCMC treated with the zinc nitrate solution was acquired. The spectrum displays similar characteristic bands of NaCMC, however, the band associated to carboxylic groups was shifted to a higher wavenumber (1612 cm^{-1}) possibly due to their strong interaction with the Zn^{2+} ions forming a Zn–CMC complex during the *in situ* precipitation process. The interactions between divalent ions and NaCMC forming complexes have been studied using FTIR analysis and a similar shift in the wavenumber of the carboxylic group absorption band has been observed (Franco et al., 2007). In addition, a strong band at 1390 cm^{-1} associated to NO_3^- ions was also observed. The FTIR spectrum of ZnS–NaCMC nanocomposite displays similar characteristic bands of Zn–CMC sample. However, after the formation of ZnS nanoparticles through the reaction between Zn^{2+} and S^{2-} ions, the carboxylic groups interacted with the Na^{2+} ions in solution shifting the stretching vibration band of carboxylic groups (COO–) at 1600 cm^{-1}, similar to that the original FTIR spectrum of sodium CMC. Based on these observations it is possible that due to the strong interaction between zinc precursor and the CMC matrix forming a complex (Zn–CMC), an electrostatic stabilization occurs during the ZnS nanoparticles precipitation trough the adsorption of NaCMC on ZnS nanocrystal surface, as can be illustrated in Fig. 1a. The vibration band assigned to NO_3^- ions was undetectable in the FTIR spectrum of ZnS–NaCMC nanocomposite which suggests that purification process can efficiently remove reaction by-products from the ZnS–NaCMC nanocomposite. ZnS does not display vibrations bands at this range of analysis.

In order to study the crystalline structure of ZnS nanoparticles deposited into the NaCMC matrix, the resulting dispersion was freeze-dried and the powders were analyzed by XRD. Fig. 2 shows the XRD patterns of NaCMC and several ZnS–NaCMC nanocomposite powders prepared using different amount of zinc precursor during *in situ* precipitation reaction labeled as S2, S3 and S4. The NaCMC diffraction pattern displays a broad peak at 20° associated with the low crystallinity of NaCMC structure that has been previously observed (Shang, Shao, & Chen, 2008). However, the diffraction patterns of ZnS–NaCMC nanocomposite powders (S2, S3 and S4) display three broad diffraction peaks at 28.95°, 48° and 58°, which agree very well with the crystallographic planes of (1 1 1), (2 2 0) and (3 1 1) in the cubic crystalline structure of ZnS (JCPD No. 77-2100). The peaks intensity of XRD pattern of S4 sample is higher than those of XRD diffraction patterns of S2 and S3 nanocomposites. This is possibly because of the amount of precursor salts added during ZnS precipitation was higher than the amount added in the rest of the experiments resulting in a higher concentration of nanocrystals. The average particle size for the S4 nanocomposite was calculated from the XRD data following the Scherrer equation (Eq. (1))

$$\langle L \rangle = \frac{0.89\lambda}{\beta \cos\theta} \quad (1)$$

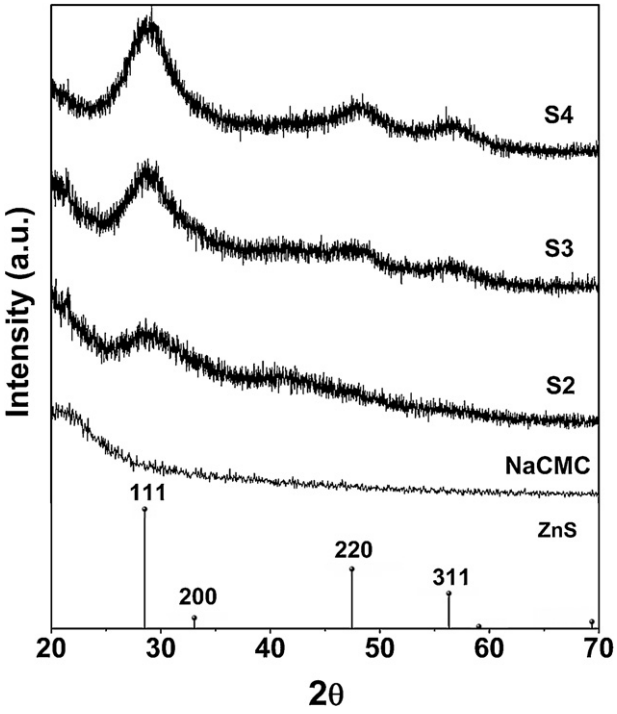

Fig. 2. XRD patterns of the NaCMC sample and the ZnS–NaCMC nanocomposites obtained with different amount of precursor salts of ZnS: S2, S3 and S4.

where λ is the wavelength of the incident X-rays, θ is the half of the diffraction angle 2θ in degrees and β is the full width at half maximum of the diffraction peak. The estimated particle size for the S2, S3 and S4 ZnS–NaCMC nanocomposites samples ranged from 1.8 to 2 nm using the FWHM of the $2\theta = 28.9°$.

3.2. Morphological characterization

In order to study the morphological characteristics of dispersed ZnS nanoparticles into NaCMC matrix, the S4 sample was analyzed by TEM and the resulting images are shown in Fig. 3. Low magnification images show a good dispersion of ZnS nanoparticles in the NaCMC evidenced by the presence of isolated nanoparticles in the observed area. This suggests that NaCMC acts as stabilizing agent during the ZnS synthesis avoiding aggregation and crystal growth. After casting, the particles remain encapsulated and well dispersed by the matrix. The particle size was measured from the TEM images and the average particle size was estimated to be 3 nm. This value is similar to that obtained using the XRD data. In addition, the HRTEM image shows a crystalline nanoparticle and lattice fringes with planar spacing of 0.311 nm which agree with the (1 1 1) planar distance in ZnS blende crystalline structure.

3.3. Optical characterization

Fig. 4 shows the optical characterization of the nanocomposite films, which was performed by acquiring transmittance spectra (Fig. 4a) and absorption spectra (Fig. 4b) in the wavelength region of 200–800 nm. The S2 and S3 ZnS–NaCMC nanocomposite films exhibit optical transmission between 90% and 70% under the visible light region. However, the optical transmission was notable decreased by increasing the amount of ZnS nanocrystals in the nanocomposite leading a transmission of 50% for the S4 nanocomposite films. On the other hand, the UV–vis absorption spectra for the nanocomposite samples (S2, S3 and S4) are shown in Fig. 4b and they display an intense absorption at 322 nm which is shifted to a shorter wavelength as compared to that of large ZnS particles (Tong

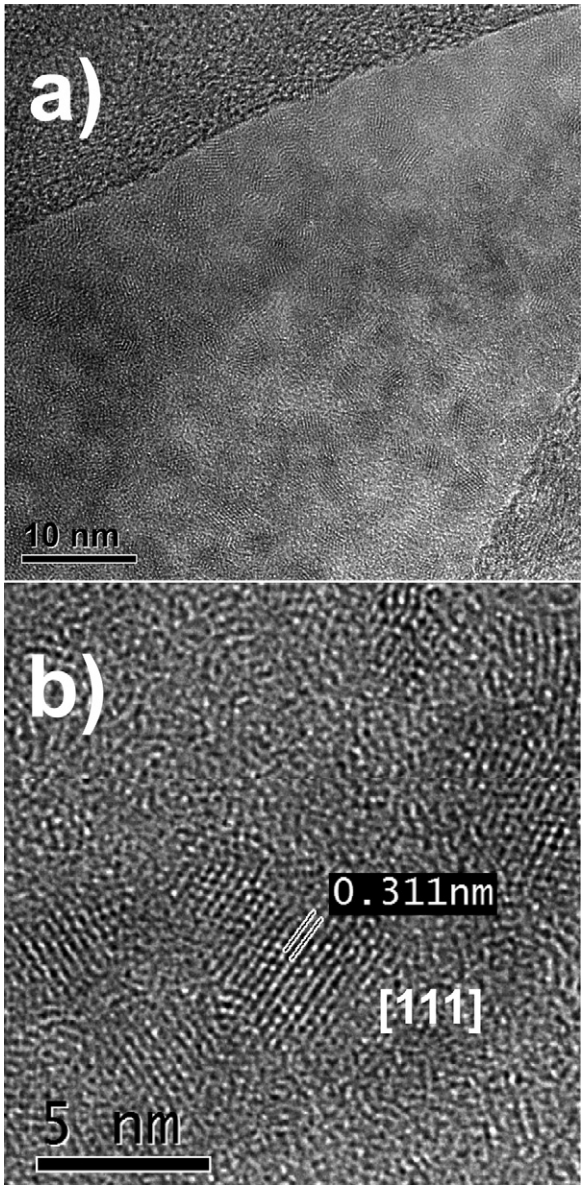

Fig. 3. TEM analysis of S4 nanocomposite. (a) Bright field image and (b) HRTEM image.

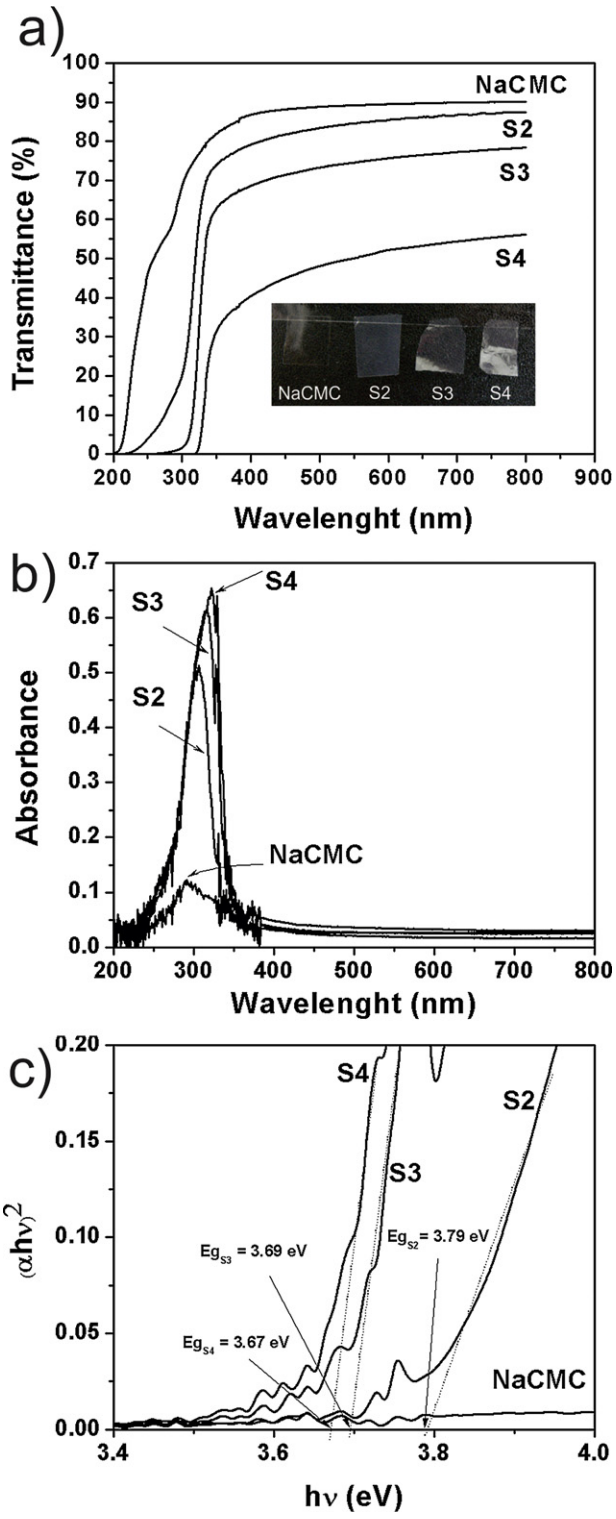

Fig. 4. Optical characterization of ZnS–NaCMC nanocomposites. (a) Transmission spectra of S2, S3 and S4, ZnS–NaCMC nanocomposite films. Inset: pictures of respective films, (b) optical absorption spectra of S2, S3 and S4, ZnS–NaCMC nanocomposite films and (c) plots of $(\alpha h\nu)^2$ vs photon energy for S2, S3 and S4, ZnS–NaCMC nanocomposite films.

et al., 2007). The optical band gap energies (Eg) for the nanocomposites prepared using different amount of precursor salts of ZnS were 3.79 eV, 3.69 eV and 3.67 eV for the S2, S3 and S4 nanocomposites respectively (Fig. 4c). The obtained direct band gap values are higher than that reported for bulk ZnS cubic crystalline structure (3.54 eV) due to the quantum confinement in the ZnS nanoparticles into NaCMC matrix (Ubale, Sangawar, & Kulkarni, 2007). In addition, the direct band gap value of the S2 nanocomposite sample is higher than those obtained for the S3 and S4 nanocomposites. This shift is possibly due to the poor crystallinity of ZnS nanoparticles in the S2 sample, which is supported by the low peak intensity in their XRD pattern. The poor crystallinity increases the number of localized states increasing the band gap energy value (Tan et al., 2005). Fig. 5 shows the room-temperature PL spectra for the several ZnS–NaCMC nanocomposite films. All nanocomposite films spectra display a broad and intense blue emission band centered at 445 nm under UV light (λ = 320 nm) excitation. The spectrum of the S4 sample shows stronger PL intensity than the spectra of S3 and S2 nanocomposite films, most likely because the amount of ZnS nanoparticles in the S4 sample is higher than for the rest of the samples resulting in a strong PL emission. This result agrees with the XRD analysis where the XRD pattern of S4 shows the strongest diffraction peak intensity which implies a high crystalline fraction in the nanocomposite film. The PL blue emission has been observed

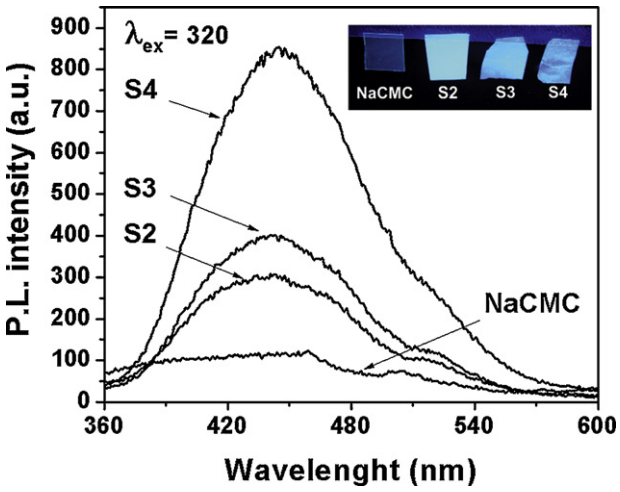

Fig. 5. PL spectra for NaCMC and S2, S3 and S4, ZnS–NaCMC nanocomposite films. Inset: pictures of nanocomposites films under UV lamp (λ = 365 nm).

in a wide variety of undoped ZnS nanostructures and it has been attributed to structural defects such as sulfur vacancies and zinc interstitial defects (Zhang, Shi, Chen, Hua, & Yan, 2001). In this case, the blue emission in the nanocomposite film is attributed to the sulfur vacancies in non-stoichiometry ZnS originated during its synthesis at room temperature. However, additional experiments should be done in order to refine this assertion.

4. Conclusions

We demonstrated photoluminescent nanocomposite films based on ZnS nanoparticles embedded in NaCMC by the *in situ* approach. The ZnS nanoparticles with sizes about 3 nm and cubic crystalline structure were deposited in the CMC matrix. The nanocomposite films showed optical transmission between 50% and 90% influenced by the amount of ZnS nanocrystals into the nanocomposite films. The optical band gap of ZnS nanoparticles was higher than that of bulk ZnS structures due to the quantum confinement. In addition, the ZnS–NaCMC nanocomposite films show a blue emission centered at 445 nm under UV light excitation (λ = 320 nm). These nanocomposites can be used in photoluminescent polymer formulations which can be easily incorporated into paper sheets in order to prepare a security paper.

Acknowledgments

The authors acknowledge the financial support by CONACYT-Mexico through the J-106365 and J-84218 projects and to UANL for its support through the PAICYT 2009 project.

References

Abitbol, T., & Gray, D. (2007). CdSe/ZnS QDs embedded in cellulose triacetate films with hydrophilic surfaces. *Chemistry of Materials*, *19*(17), 4270–4276.

Arachchige, I. U., & Brock, S. L. (2007). Highly luminescent quantum-dot monoliths. *Journal of the American Chemical Society*, *129*(7), 1840–1841.

Basta, A. H., & El-Saied, H. (2008). New approach for utilization of cellulose derivatives metal complexes in preparation of durable and permanent colored papers. *Carbohydrate Polymers*, *74*(2), 301–308.

Calandra, P., Longo, A., & Liveri, V. T. (2003). Synthesis of ultra-small ZnS nanoparticles by solid-solid reaction in the confined space of AOT reversed micelles. *Journal of Physical Chemistry B*, *107*(1), 25–30.

Chang, C., Peng, J., Zhang, L., & Pang, D.-W. (2009). Strongly fluorescent hydrogels with quantum dots embedded in cellulose matrices. *Journal of Materials Chemistry*, *19*(41), 7771–7776.

Franco, A. P., Lobo-Recio, M. A., Szpoganicz, B., López-Delgado, A., Felcman, J., & Romalho-Merce, A. L. (2007). Complexes of carboxymethylcellulose in water. Part 2. Co^{2+} and Al^{3+} remediation studies of wastewaters with Co^{2+}, Al^{3+}, Cu^{2+}, VO^{2+} and Mo $^{6+}$. *Hydrometallurgy*, *87*(3–4), 178–189.

Generalova, A. N., Sizova, S. V., Oleinikov, V. A., Zubov, V. P., Artemyev, M. V., Spernath, L., et al. (2009). Highly fluorescent ethyl cellulose nanoparticles containing embedded semiconductor nanocrystals. *Colloids and Surfaces A: Physicochemical and Engineering Aspects*, *342*(1–3), 59–64.

Gruzintsev, A. N., Emelchenko, G. A., Masalov, V. M., Yakimov, E. E., Barthou, C., & Maitre, A. (2009). Luminescence of CdSe/ZnS quantum dots infiltrated into an opal matrix. *Semiconductors*, *43*(2), 197–201.

Guo, L., Chen, S., & Chen, L. (2007). Controllable synthesis of ZnS/PMMA nanocomposite hybrids generated from functionalized ZnS quantum dots nanocrystals. *Colloid and Polymer Science*, *285*(14), 1593–1600.

Hebalkar, N., Lobo, A., Sainkar, S. R., Pradhan, S. D., Vogel, W., Urban, J., et al. (2001). Properties of zinc sulphide nanoparticles stabilized in silica. *Journal of Materials Science*, *36*(18), 4377–4384.

Kuiri, P. K., Ghatak, J., Joseph, B., Lenka, H. P., Sahu, G., Mahapatraa, D. P., et al. (2007). Effect of Au irradiation energy on ejection of ZnS nanoparticles from ZnS film. *Journal of Applied Physics*, *101*(1), 014313.

Li, X., Chen, S., Hu, W., Shi, S., Shen, W., Zhang, X., et al. (2009). In situ synthesis of CdS nanoparticles on bacterial cellulose nanofibers. *Carbohydrate Polymers*, *76*(4), 509–512.

Mu, J., Gu, D., & Xu, Z. (2005). Synthesis and stabilization of ZnS nanoparticles embedded in silica nanospheres. *Applied Physics A*, *80*(7), 1425–1429.

Pandey, S., & Pandey, A. C. (2009). Optical properties of hybrid composites based on highly luminescent CdS and ZnS nanocrystals in different polymer matrices. In *Transport and Optical Properties of Nanomaterials—ICTOPON-2009, vol. 1147, no. 1* (pp. 216–222).

Qi, H., Chang, C., & Zhang, L. (2009). Properties and applications of biodegradable transparent and photoluminescent cellulose films prepared via a green process. *Green Chemistry*, *11*(2), 177–184.

Rosseti, R., Ellison, J. L., Gibson, J. M., & Brus, L. E. (1984). Size effects in the excited electronic states of small colloidal CdS crystallites. *Journal of Chemical Physics*, *80*(9), 1.

Rozenberg, B. A., & Tenne, R. (2008). Polymer-assisted fabrication of nanoparticles and nanocomposites. *Progress in Polymer Science*, *33*(1), 40–112.

Ruan, D., Huang, Q., & Zhang, L. (2005). Structure and properties of CdS/regenerated cellulose nanocomposites. *Macromolecular Materials and Engineering*, *290*(10), 1017–1024.

Shang, J., Shao, Z., & Chen, X. (2008). Electrical behavior of a natural polyelectrolyte hydrogel:chitosan/carboxymethylcellulose hydrogel. *Biomacromolecules*, *9*(4), 1208–1213.

Shen, J., Song, Z., Qiana, X., & Yang, F. (2010). Carboxymethyl cellulose/alum modified precipitated calcium carbonate fillers: Preparation and their use in papermaking. *Carbohydrate Polymers*, *81*(3), 545–553.

Tan, S. T., Chen, B. J., Sun, X. W., Fan, W. J., Kwok, H. S., Zhang, X. H., et al. (2005). Blueshift of optical band gap in ZnO thin films grown by metal-organic chemical-vapor deposition. *Journal of Applied Physics*, *98*(1), 013505.

Tong, H., Zhu, Y., Yang, L., Li, L., Zhang, L., Chang, J., et al. (2007). Self-assembled ZnS nanostructured spheres: Controllable crystal phase and morphology. *Journal of Physical Chemistry C*, *111*(10), 3893–3900.

Ubale, A. U., Sangawar, V. S., & Kulkarni, D. K. (2007). Size dependent optical characteristics of chemically deposited nanostructured ZnS thin films. *Bulletin of Material Science*, *30*(2), 147–151.

Velumani, S., & Ascencio, J. A. (2004). Formation of ZnS nanorods by simple evaporation technique. *Applied Physics A*, *79*(1), 153–156.

Vimala, K., Samba Sivudu, K., Murali Mohan, Y., Sreedhar, B., & Mohana Raju, K. (2009). Controlled silver nanoparticles synthesis in semi-hydrogel networks of poly(acrylamide) and carbohydrates: A rational methodology for antibacterial application. *Carbohydrate Polymers*, *75*(3), 463–471.

Xu, J. F., Ji, W., Lin, J. Y., Tang, S. H., & Du, Y. W. (1998). Preparation of ZnS nanoparticles by ultrasonic radiation method. *Applied Physics A*, *66*(6), 639–641.

Zhang, W., Shi, J., Chen, H., Hua, Z., & Yan, D. (2001). Synthesis and characterization of nanosized ZnS confined in ordered mesoporous silica. *Chemistry of Materials*, *13*(2), 648–654.

Zhu, J., Zhou, M., Xu, J., & Liao, X. (2001). Preparation of CdS and ZnS nanoparticles using microwave irradiation. *Materials Letters*, *47*(1–2), 25–29.